

Article

Identification of Potential Non-Systemic Therapeutics for Hyperammonemia

Brad Nicklas ¹, Simon Velasquez Morales ^{1,2,3}, Jian Qian ⁴, Kyle J. Stephens ^{1,2,3}, David R. Corbin ³, Mark B. Shiflett ^{1,3}, Cory J. Berkland ^{1,4} and Alan M. Allgeier ^{1,2,3,*}

¹ Department of Chemical & Petroleum Engineering, University of Kansas, Lawrence, KS 66045, USA

² Center for Environmentally Beneficial Catalysis, University of Kansas, Lawrence, KS 66045, USA

³ Institute for Sustainable Engineering, University of Kansas, Lawrence, KS 66045, USA; david.r.corbin@ku.edu

⁴ Department of Pharmaceutical Chemistry, University of Kansas, Lawrence, KS 66047, USA

* Correspondence: alan.allgeier@ku.edu

Abstract: A non-absorbable therapeutic candidate for the treatment of hyperammonemia has been identified and characterized. Conventional approaches to reducing ammonia concentration in the blood and colon include acidifying the colon, inhibiting the bacterial production of ammonia, and activation of the urea cycle. Addressing gaps in the literature around therapeutic ammonia adsorption, this study established assays for ammonia uptake from both NH_4OH and NH_4Cl solutions as well as interference and selectivity for potassium absorption. Performance was characterized for a large number and variety of materials, spanning zeolites, ion-exchange resins, metallopolymers, metal–organic frameworks (MOFs), and polymeric carboxylic acids. The latter class showed low potassium capacity (poly(acrylic acid): 10 mg/g, poly(maleic-co-acrylic acid): 4 mg/g) and a therapeutically relevant depression of pH in buffered simulated intestinal fluid (SIF) (poly(acrylic acid): -2.01 and poly(maleic-co-acrylic acid): -3.23) compared to lactulose (-3.46), an approved therapeutic for hyperammonemia that works by acidifying the colon. In the polymeric organic acids evaluated, pH depression correlated well with pKa and acid site density. Additionally, this class of candidates should avoid the undesirable side effects of lactulose, such as the potential for hyperglycemia in diabetic patients and incompatible use with galactosemic patients.

Keywords: hyperammonemia; zeolites; ion-exchange resins; polymeric organic acids; metallopolymers; metal–organic frameworks (MOFs); colon



Citation: Nicklas, B.; Velasquez Morales, S.; Qian, J.; Stephens, K.J.; Corbin, D.R.; Shiflett, M.B.; Berkland, C.J.; Allgeier, A.M. Identification of Potential Non-Systemic Therapeutics for Hyperammonemia. *Drugs Drug Candidates* **2023**, *2*, 796–809. <https://doi.org/10.3390/ddc2040040>

Academic Editors: Jean Jacques Vanden Eynde and Marco Bruno Luigi Rocchi

Received: 26 July 2023

Revised: 18 September 2023

Accepted: 20 September 2023

Published: 30 September 2023



Copyright: © 2023 by the authors. Licensee MDPI, Basel, Switzerland. This article is an open access article distributed under the terms and conditions of the Creative Commons Attribution (CC BY) license (<https://creativecommons.org/licenses/by/4.0/>).

1. Introduction

Hyperammonemia, a metabolic disease characterized by elevated ammonia levels in the blood, causes neurological disorders, including cognitive impairment, ataxia, and coma [1]. One secondary complication is hepatic encephalopathy (HE) as the liver cannot remove all the excess ammonia, and the toxic compound ultimately causes disruption between neurons and astrocytes in the brain [1]. The 3-year survival rate for severe HE with hyperammonemia is 23% [1]. One of the most common causes of hyperammonemia, urea cycle defect (UCD), occurs in 1 of every 250,000 births in the US [1]. The 11-year survival rate for early-onset hyperammonemia caused by UCD is 35% [1], underscoring the urgency for treatment of the disorder, particularly in children.

Most bodily ammonia is produced through protein digestion and bacterial metabolism in the colon, followed by diffusion to the bloodstream [2]. Typical blood ammonia concentrations vary depending on age and urea cycle efficiency, with 50 μM being the typical maximum for healthy adults [2], while neonatal patients may normally experience 70–90 μM [1]. Normally, excess ammonia is catabolized in chemical pathways, and nitrogenous waste is converted into urea via the urea cycle [2]. Free ammonia (NH_3) is highly toxic in the blood, while ammonium (NH_4^+) cannot diffuse readily through the intestinal wall into the

obstacle for selective binding because of its similar properties to ammonia, including equal ionic charge and roughly equal hydration radius and energy [12].

To our knowledge, there is no reported use of non-absorbable treatments using MoA1 in the treatment of hyperammonemia. Current treatments for the disease focus on the acidification of the colon and the inhibition of ammonia-producing colonic bacteria [2]. Lactulose, the current first-line therapy for hyperammonemia, undergoes metabolism by enteric bacteria to produce lactic and acetic acids, decreasing colon pH (MoA1) [13]. Drawbacks of this therapy include: (1) adverse effects, (2) incompatibilities with several patient populations, and (3) large dose. Adverse effects comprise the sensation of bloating, increased flatulence, increased bowel sounds, nausea, electrolyte imbalance, and most significantly, diarrhea [14]. Further, lactulose cannot be used by patients with galactosemia as galactose is one product of lactulose metabolism in the gut [15]. Although lactulose is largely non-systemic, there have been reported cases of it causing hyperglycemia in diabetic patients [14]. Pregnant patients have experienced electrolyte imbalance upon extended use [14]. Lactulose requires large doses, with a bolus of 30 g being administered hourly for HE episodes until the episode subsides, and the dose is titrated for each patient [14].

Here, we evaluate the performance of a wide range of candidate, non-absorbable therapeutics for the treatment of hyperammonemia either via ammonia adsorption/sequestration or pH adjustment. Candidate materials span zeolites, ion-exchange resins, metallopolymers, metal-organic frameworks (MOFs), and polymeric organic acids.

2. Results and Discussion

2.1. Zeolites

Zeolites were the initial target of screening for MoA1 due to their broad commercial availability, high ion-exchange site density, range of structures/acidities, and larger densities compared to polymeric resins. At equal performance, a larger density implies a smaller volumetric dose, enhancing patient experience. Ten zeolites were initially tested in 50 mM NH_4OH (initial pH = 11) to determine ammonia binding capacity. Despite the moniker NH_4OH , at this pH, the majority of ammonia present is in the unprotonated NH_3 form. A range of structure types and Si:Al ratios (5.1–80 for CBV zeolites) were evaluated. All CBV zeolites have the same structure (faujasite) but differ based on ion-exchange content. A subset of samples, each representing a different framework structure, was further characterized for the adsorption of NH_4Cl (aq, pH = 6.43). Since ammonia is primarily in the protonated form in such solutions, NH_4^+ adsorption necessitates ion exchange, releasing a bound proton, alkali, or alkaline earth cation into the solution. All except clinoptilolite exhibited a decrease in binding capacity when tested in chloride solution (Figure 2). This is logical because all the zeolites tested for NH_4Cl adsorption were in the acid form, except clinoptilolite, which comprises sodium, potassium, and calcium instead of protons. It is clear that zeolitic protons do not easily exchange with NH_4^+ .

Changes in pH (MoA2) were also measured for the subset of six zeolites to assess the impact the material would have on the acidification of the colon. All materials except clinoptilolite decreased the pH, consistent with the above discussion of ion exchange (Figure 3). Of the five zeolites that did decrease the pH, all but Cu-4A exhibited larger decreases in the ammonium chloride solution than the ammonium hydroxide solution (Figure 3).

The capacities of zeolites have been extensively reported in the wastewater treatment literature [16]. Literature reports of the ammonia binding capacity of clinoptilolite, one of the most abundant and researched zeolites, vary significantly [17]. The present values are reasonable in light of reported values in the range of 2.7 to 30.6 mg/g [18,19].

The impact of pH is largely underreported in the literature, with pH data primarily concerning the effect of the initial pH on adsorption, rather than any effect the adsorbent has on the solution. The latter is a critical aspect of hyperammonemia treatment.

Approximate dosages based on ammonia capacities were calculated using the conservative assumptions of 5 mM ammonia in the colon and full adsorption

(Supplementary Materials), though clinical improvement is expected with even fractional adsorption [20]. The lowest estimated dosage of the zeolites tested was 16.7 g/day.

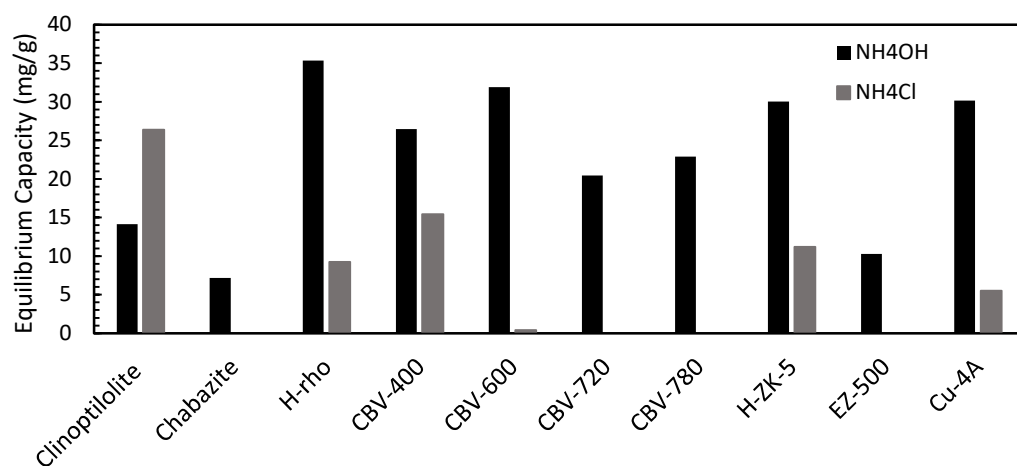


Figure 2. Ammonia equilibrium capacities of zeolites in aqueous ammonia solutions.

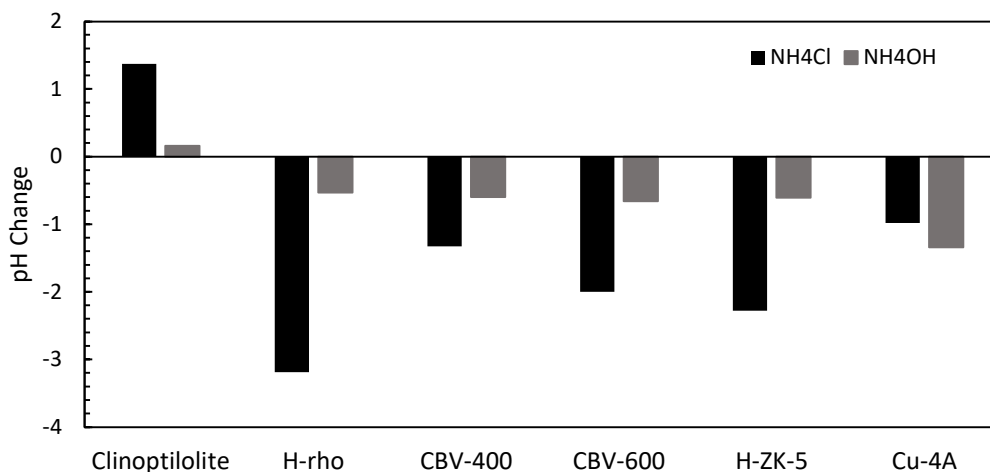


Figure 3. Changes in pH caused by zeolites in aqueous solutions.

2.2. Ion-Exchange Resins

Ion-exchange resins have high capacities for removing ions from solutions (MoA1). Additionally, acidic ion-exchange resins may protonate ammonia, acidifying the colon and thus shifting the equilibrium away from NH₃ (MoA2).

Six ion-exchange resins were tested: a strong basic anion resin (Dowex 1×2-200 chloride form), a sulfonated tetrafluoroethylene-based fluoropolymer-copolymer (Nafion 1080 × R H⁺ form), a polysiloxane-supported alkyl sulfonic acid (Deloxan ASP 1/9), and three strong acidic cation exchangers (Amberlite IR-120 H⁺ form, C100E, and C100EH) were tested in NH₄OH. The four materials with the highest capacity were also tested in NH₄Cl.

Strong acidic cation-exchange resins in the H⁺ form were far superior in ammonia capacity over other ion-exchange resins and zeolites tested (Figure 4). Both strong acidic H⁺ form resins demonstrated a decrease in ammonia capacity in the more neutral NH₄Cl solution (pH ≈ 6.5) compared to the basic NH₄OH (pH ≈ 11) solution (Figure 4).

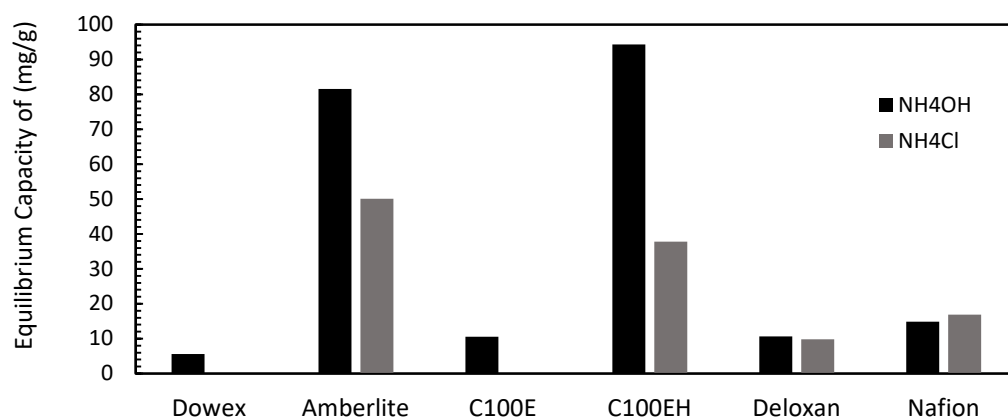


Figure 4. Ammonia equilibrium adsorption capacities of ion-exchange resins. (Dowex and C100E not tested in NH₄Cl due to poor performance in NH₄OH).

Changes in pH (MoA2) were also characterized. Strong acidification was seen in NH₄Cl, and some acidification was seen in NH₄OH for H⁺ form resins (amberlite, C100EH, Deloxan, and Nafion), whereas little to no decrease was seen in Dowex and C100E (Figure 5). These two resins were supplied in the Cl⁻ and Na⁺ forms, respectively. Accordingly, they had little potential to decrease pH.

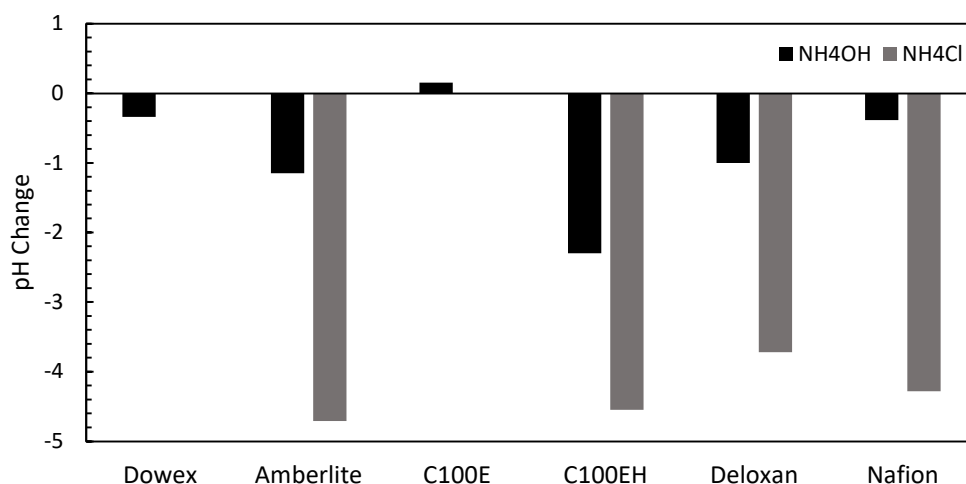


Figure 5. Changes in pH caused by ion-exchange resins in aqueous ammonia solutions. (Dowex and C100E were not tested in NH₄Cl due to poor performance in NH₄OH).

The literature scope on ion-exchange resins is similarly broad as that of zeolites, focuses on wastewater treatment, and lacks standardization across studies, making it difficult to compare materials from different studies [17,18,21]. The largest capacity in NH₄Cl across all zeolites and ion-exchange resins in this study was 50 mg/g, yielding a conservatively estimated dose of 11.8 g/day. Acknowledging that therapeutic benefit may be realized at a fraction of this dose, it became important to assess adsorption selectivity, particularly the selectivity of ammonia over K⁺ (Figure 6). Cross-linked poly(acrylic acid) was evaluated for the comparison of carboxylic acid to sulfonic acid groups of C100EH, which have a lower pKa than carboxylic acids. It was determined that the degree of cross-linking did not affect equilibrium binding capacity (Supplementary Materials). Samples were tested in an equimolar solution of KCl and NH₄Cl. Under these conditions, the strong acid, C100EH, experienced a dramatic decrease in ammonia binding capacity: <6 mg/g compared to 59.8 mg/g in the absence of KCl. Simultaneously, K⁺ bound more selectively, reaching 59 mg/g. Poly(vinyl sulfonic acid) was synthesized and evaluated in the assays and exhibited very similar trends to C100EH with respect to ammonia binding and K⁺

selectivity (Supplementary Materials). This large selectivity for K^+ represents a major drawback, making C100EH unsuitable for the treatment of hyperammonemia. Similar behavior is anticipated for other strongly acidic ion-exchange resins, due to the similar shape and size of K^+ and NH_4^+ ions [22].

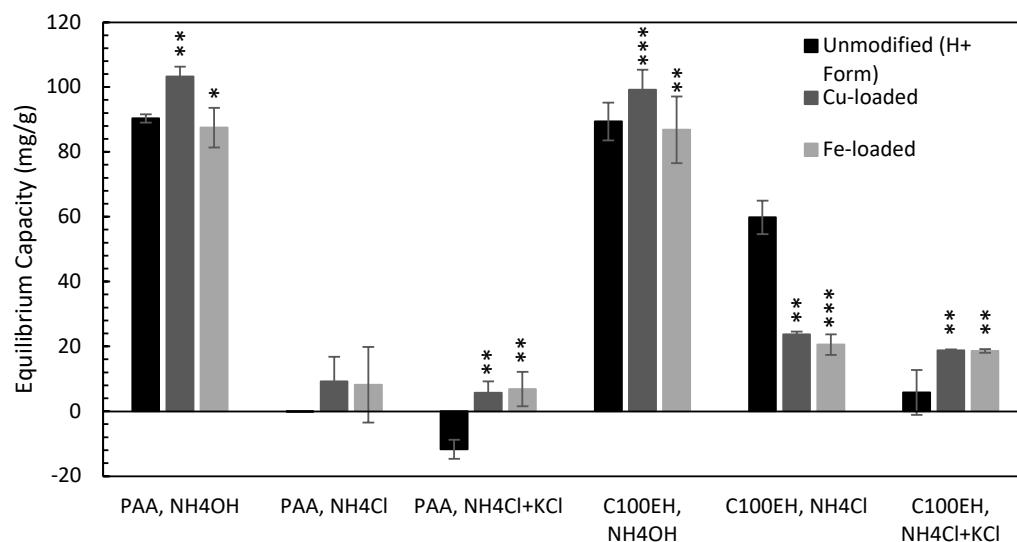


Figure 6. Ammonia equilibrium capacities for modified and unmodified PAA and C100EH in aqueous ammonia solutions. (No error bars were generated for PAA in NH_4Cl). *** $p < 0.001$; ** $0.001 \leq p \leq 0.05$; * $p > 0.05$ student's *t*-test two-tailed paired.

2.3. Metal Complexes

To address the K^+ selectivity challenge, an orthogonal approach based on metal–ammonia binding compounds was pursued. It was hypothesized that the dative bond formed when ammonia shares electrons with a metal ion would engender greater selectivity for ammonia adsorption in the presence of potassium. Copper and iron variants were evaluated, with both metals being loaded onto cross-linked poly(acrylic acid) and C100EH via ion exchange.

For Cu-PAA and Cu-C100EH samples, ammonia capacity generally increased relative to unmodified resins (Figure 6). Composition analyses of metal-loaded resins by X-ray fluorescence are reported in the Supplementary Materials. The Cu loading on PAA was 0.5 meq/g and the Fe loading on PAA reached 1.1 meq/g, and the adsorption capacity of each metal-loaded resin is approximately the same value within error. Further, the metal-loaded PAA retained ammonia adsorption capacity even in the presence of competing K^+ ions. By comparison, when unmodified PAA was exposed to NH_4Cl solution, it did not adsorb ammonia/ammonium (the capacity was measured as -0.2 mg/g and is present but not resolved in Figure 6). PAA has a theoretical acid density of 13.9 meq/g and when exposed to basic ammonia solution adsorbs 5.3 meq/g. Clearly, the metal exchange represents a fraction of the total sites available.

Accordingly, the decrease in pH upon resin exposure (Figure 7) is barely affected by metal loading for PAA. While such resin modification offers a slight benefit, the performance remains dominated by the acid sites of the resin. In comparison to PAA, C100EH, with its phenyl sulfonic acid sites, has a lower pKa and yields a substantially larger decrease in solution pH compared to PAA (Figure 7). The unmodified resin is produced at an accessible acid site density of 1.9 meq H^+ /g and yet, adsorbed 3.5 meq NH_3 /g in the basic ammonia (NH_4OH) assay. The Cu loading on C100EH was 0.5 meq/g and the Fe-loaded sample reached 0.9 meq/g. These values are nearly identical to the PAA loading, but the percentage of acid sites exchanged with metal ions is much larger in C100EH than in PAA. Accordingly, the pH decrease is significantly impacted for metal ion-exchanged C100EH samples (Figure 7). Metal-C100EH samples reached larger capacities in NH_4Cl solution

than the corresponding PAA resins even though metal loading was nearly identical. This suggests that adsorption is attributable to both acid and metal sites. The stronger acid sites of C100EH are available for NH_4^+ exchange, whereas the weaker acid sites of PAA do not promote NH_4^+ binding. As with the PAA variants, metal-loaded C100EH resins displayed an increase in the ratio of NH_4^+ to K^+ binding compared to unmodified resin, in competitive adsorption tests, as hypothesized.

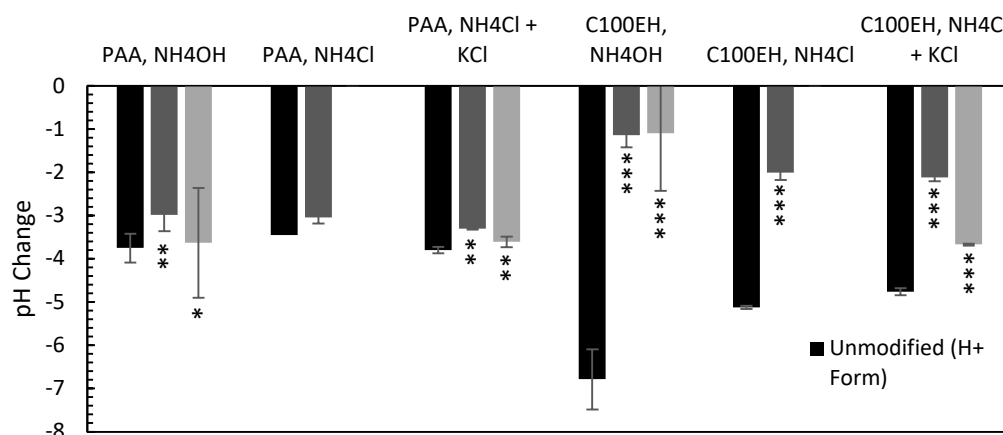


Figure 7. Changes in pH caused by modified and unmodified PAA and C100EH in aqueous ammonia solutions. (Fe-loaded PAA and C100EH not measured in NH_4Cl). *** $p < 0.001$; ** $0.001 \leq p \leq 0.05$; * $p > 0.05$ student's *t*-test two-tailed paired or homoscedastic (Fe-loaded PAA in NH_4OH only).

All metal-loaded materials increased ammonia capacity in the equimolar $\text{NH}_4\text{Cl}/\text{KCl}$ assay with respect to their unmodified H^+ forms (Figure 8). The potassium capacity was decreased in the metal-loaded C100EH sample, whereas Cu and Fe increased the potassium capacity in PAA. Although the potassium capacity of any material was not decreased enough to be of therapeutic value, the Fe-PAA and Fe-C100EH were both slightly selective for NH_4^+ .

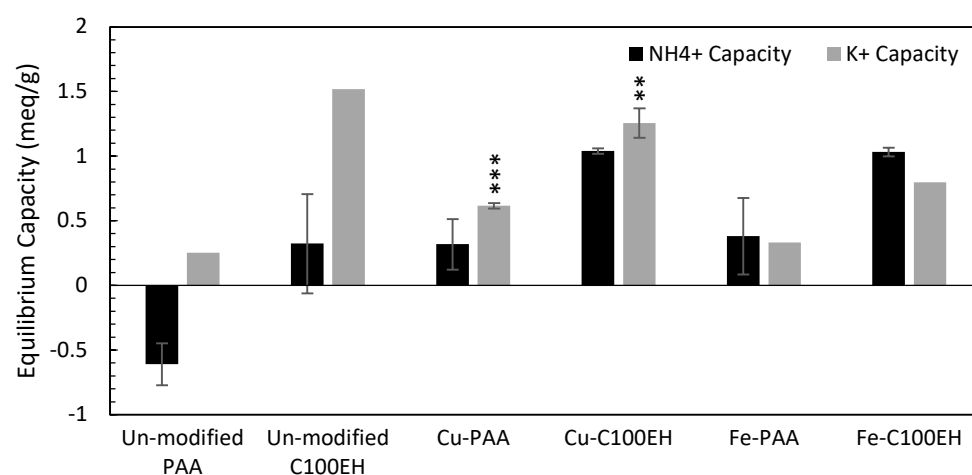


Figure 8. Ammonia and potassium equilibrium capacities of modified and unmodified PAA and C100EH in equimolar $\text{KCl} + \text{NH}_4\text{Cl}$ solution. *** $p < 0.001$; ** $0.001 \leq p \leq 0.05$ student's *t*-test two-tailed paired (Cu-PAA) or homoscedastic (Cu-C100EH).

This trend of selectivity for ammonia over potassium adsorption on transition metal-loaded adsorbents is in line with a report by Clark and Tarpeh, who reported an ammonia capacity as high as 8 meq/g and an N/K selectivity as high as 10.1 in equimolar solutions using transition metal-loaded polymeric cation-exchange resins under optimized conditions [12].

2.4. Metal–Organic Frameworks

Two metal–organic frameworks (MOFs), Fe-BTC and Cu-BTC, were also screened. MOFs hold similar advantages of zeolites in that they possess large surface areas and have a high degree of tunability, due to the sheer number of compounds that can be used to assemble MOFs.

Overall, both MOFs had a small ammonia capacity, which would not make them attractive treatments, with the highest capacity being 25 mg/g, resulting in an estimated dosage of 23.6 g (Figure 9). In one case, the capacity was so low that the uncertainty was very large. However, an interesting trend was seen in Cu-BTC that was not seen in other materials. A larger capacity for ammonia was seen in chloride solutions than in the NH₄OH solution. Furthermore, a higher capacity for ammonia was seen in the solution also containing potassium (Figure 9). This could mean that as the total concentration of the ions in solution increases, the ammonia/ammonium equilibrium is shifted, as is the selectivity for Cu binding ammonia versus water, as seen by Clark and Tarpeh [12].

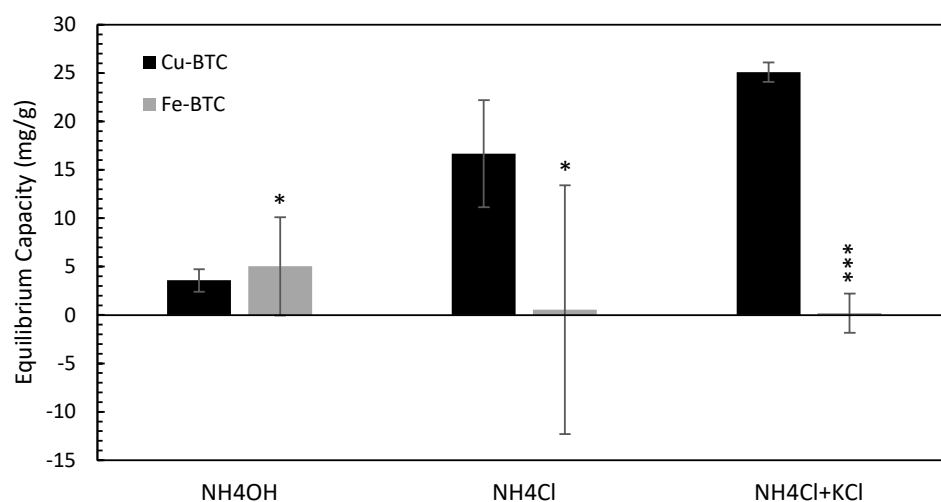


Figure 9. Ammonia equilibrium capacities of Cu-BTC and Fe-BTC in aqueous ammonia solutions. *** $p < 0.001$; * $p > 0.05$ student’s *t*-test two-tailed paired.

The pH changes seen in the MOF were less than for C100EH (Figure 7, unmodified form; Figure 10). This means that MOFs are likely not a suitable candidate for the pH change treatment approach (MoA2), as they should experience even less pH change in a buffered solution like the colon.

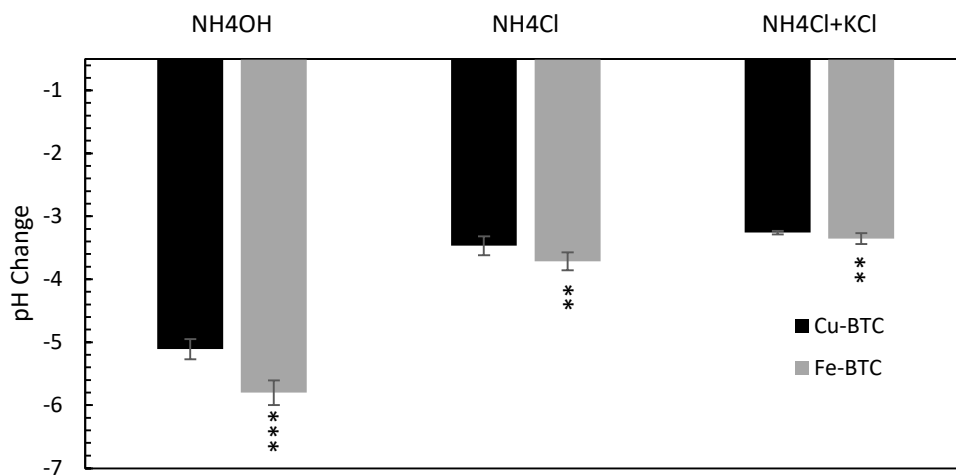


Figure 10. Changes in pH caused by Cu-BTC and Fe-BTC in aqueous ammonia solutions. *** $p < 0.001$; ** $0.001 \leq p \leq 0.05$ student’s *t*-test two-tailed paired.

2.5. Modification of Polymeric Organic Acids

Acknowledging that PAA has low affinity for potassium but also low capacity for NH_4^+ adsorption, we sought to improve selectivity by evaluating poly(maleic acid) (PMA). PMA has a higher acid site density and a lower pKa than PAA. Since these polymers bear carboxylic acid functional groups that could acidify the colon, it was appropriate to draw comparisons to the lactulose therapy. The exact mechanism of lactulose is still unproven, although it is currently suggested to be digested by colonic bacteria (Figure 11) [14]. By acidifying the colon, the equilibrium is shifted away from toxic NH_3 and towards NH_4^+ , which cannot be absorbed through the colon and into the bloodstream. Additionally, the acidification of the colon discourages the formation of urease-active bacteria while encouraging the growth of acid-resistant non-urease bacteria [2]. The enzyme urease breaks down urea into NH_3 , hence inhibiting urease inhibits the formation of ammonia. An initial estimate was based on the known acids that resulted from the breakdown of lactulose [2].

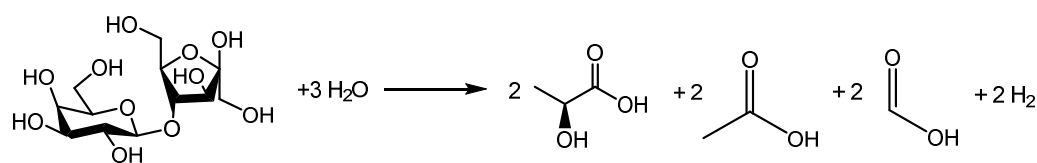


Figure 11. Potential digestion of lactulose into lactic acid, acetic acid, and formic acid [13].

To provide an upper-bound estimate for the effects of lactulose, the assumed stoichiometry in Figure 11 was used to synthesize simulated lactulose digestion product using two equivalents each of lactic acid, acetic acid, and formic acid for each equivalent of lactulose. Actual acid equivalent generation is likely lower in vivo due to the complexity and inefficiency of digestion [13]. Furthermore, the performance of the simulated lactulose digestion product was evaluated using simulated colonic fluid (fed state), prepared by the method of Marques et al. [23]. Since lactic, acetic, and formic acids are soluble in water, a low-molecular-weight, water-soluble PAA was evaluated to assess any effect solubility had on acidification. A copolymer of PMA and PAA (poly(acrylic acid-co-maleic acid, PAACMA) with a co-monomer ratio of 1:1 was also tested since the copolymer had a higher molecular weight, which allowed for separation via dialysis tubes to analyze if the material had undesired potassium selectivity. Even water-soluble polymers may be therapeutically relevant if their molecular weight precludes bloodstream absorption.

PMA had the highest acidification of all acids tested in simulated colonic fluid, consistent with its low pKa = 1.83 [24] (Figure 12). Simulated lactulose was slightly less acidifying than PMA (≈ 0.5 higher pH), with PAACMA slightly less than simulated lactulose. PAACMA was halfway between soluble PAA and PMA, consistent with the 1:1 co-monomer ratio. Cross-linked PAA was slightly less acidifying than the soluble version.

Table 1. Coefficients and statistical values for Figure 12.

Material	a	b	Adjusted R-Squared	p-Value (a)	p-Value (b)
PMA	−1.05	−0.88	0.98	9.6×10^{-5}	1.8×10^{-3}
X-linked PAA	−0.39	−0.69	0.92	1.7×10^{-3}	2.3×10^{-3}
Simulated Lactulose	−0.74	−1.42	0.94	8.9×10^{-4}	7.9×10^{-4}
Soluble PAA	−0.49	−0.65	0.88	3.7×10^{-4}	1.3×10^{-3}
PAACMA	−0.88	−0.68	1.00	2.7×10^{-8}	6.7×10^{-6}

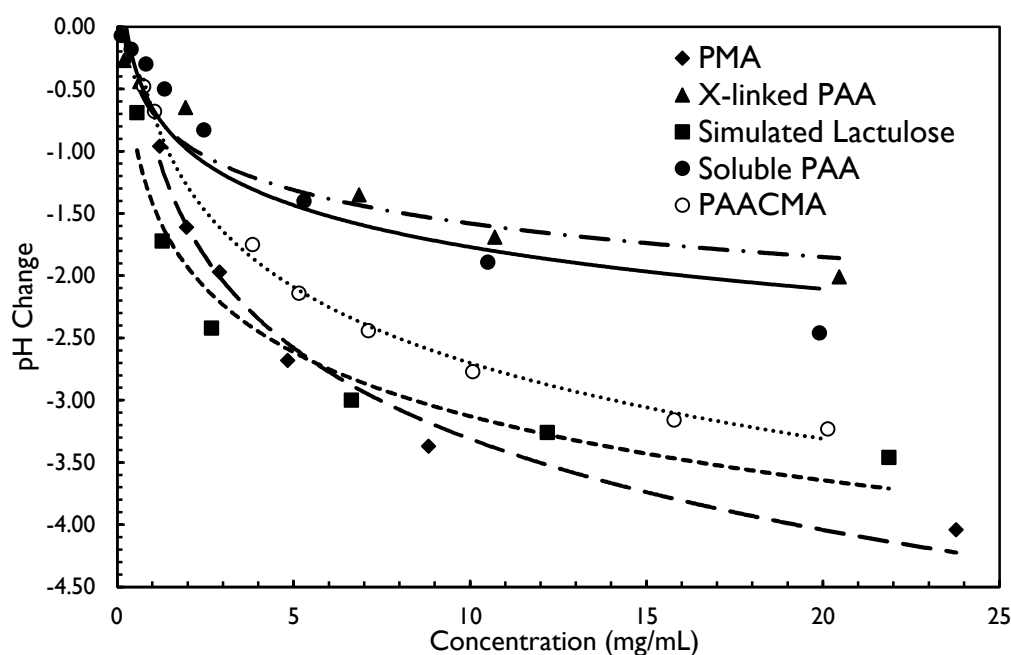


Figure 12. pH changes caused by organic polymeric acids and lactulose in simulated colonic fluid. Curves were generated using the least-squares method. Characteristics of the regression $y = a \times \ln(x) + b$ for each data set is given in Table 1.

PAACMA exhibited an equilibrium potassium capacity (4 mg/g) that was quite similar to 5% cross-linked PAA (10 mg/g), further supporting the potential of this class of non-absorbable therapeutics for the treatment of hyperammonemia. It is further noted that while PAA and PAACMA do not appear on the U.S. Food and Drug Administration's list of Generally Recognized as Safe ingredients, comparable small molecules including malic and succinic acid do have this designation. It is likely that the polymers will be characterized as non-toxic in follow-up studies. Of additional note, the in vivo assay with simulated colonic fluid used in this study is deemed a first step in generating hyperammonemia therapies, and in vitro studies are necessary for further development.

3. Materials and Methods

3.1. Materials

Samples of zeolite H-Y (CBV-400, CBV-600, CBV-720, CBV-780) were used as received from Zeolyst (Conshohocken, PA, USA). EZ-500 (ferrierite) was used as received from Engelhard Corporation (Iselin, NJ, USA) (now BASF (Ludwigshafen, Germany)). C100E and C100EH were used as received from Purolite (Upper Merion Township, PA, USA). Deloxan ASP 1/9 was used as received from Degussa (Berlin, Germany) (now Evonik (Essen, Germany)). Amberlite IR-120 (+) ion-exchange resin, Dowex 1×2-200 ion-exchange resin, Trizma Base (crystalline, ≥99% (titration)), poly(acrylic acid-co-maleic acid) solution (average M_w 3000, 50 wt. % in H_2O), Cu-BTC (Basolite C300, produced by BASF), Fe-BTC (Basolite F300, produced by BASF), ammonium chloride (ACS reagent, ≥99.5%), poly(acrylic acid) (average M_w 1800), bovine serum albumin (heat shock fraction, pH 7, ≥98%), N,N'-methylenebisacrylamide (powder, for molecular biology, for electrophoresis, ≥99.5%), acrylic acid (anhydrous, contains 200 ppm MEHQ as inhibitor, 99%), phenol (puriss. p.a., ACS reagent, reagent grade, Ph. Eur., 99.0–100.5%), ammonium hydroxide solution (ACS reagent, 28.0–30.0% NH_3 basis), potassium chloride (for molecular biology, ≥99.0%), hydrogen chloride (ACS reagent, 37%), N,N-dimethylformamide (for HPLC ≥99.9%), 2,2'-azobis(2-methyl-propionamide) dihydrochloride (granular, 97%), sodium hydroxide (reagent grade, ≥98%, pellets (anhydrous)), and D-(+)-glucose (≥99.5%, GC) were used as received from Sigma Aldrich (St. Louis, MO, USA). Sodium hypochlorite solution (laboratory grade 5.65–6%), ethyl alcohol (95% denatured with IPA and methanol), were

used as obtained from Fisher Scientific (Waltham, MA, USA). Iron (II) sulfate heptahydrate (99+%, ACS reagent) was used as received from Acros Organics (Waltham, MA, USA). Copper (II) sulfate hydrate pentahydrate (USP) was used as received from J.T. Baker (Phillipsburg, NJ, USA). Sodium pentacyanonitrosylferrate (III) dihydrate was used as received from Alfa Aesar (Haverhill, MA, USA). Poly(maleic acid) (48% aqueous solution) was used as received from Biosynth (Gardner, MA, USA). Lactic acid (10% *v/v*) was used as received from Ricca Chemical Company (Arlington, TX, USA). Acetic acid (10% aqueous solution) was used as received from Ward's Science (Rochester, NY, USA). Clinoptilolite from KMI Zeolite (Pahrump, NV, USA) was calcined at 400 °C. Chabazite (Durkee, OR, USA) from Mineral Research was sieved to -20/+40 mesh. Nafion 1080 × R H⁺ Form Ground to 35–60 Mesh was used as received from DuPont (Wilmington, DE, USA). Sodium vinylsulfonate was used as received from TCI Chemicals (Portland, OR, USA). ZK-5 and rho zeolites were prepared using methods from the literature, followed by ammonium ion exchange using conventional methods, and subsequently, they were calcined to generate the hydrogen forms [25,26].

3.2. Measurements

The Berthelot reaction was used to assay total nitrogen present as NH₃ or NH₄⁺ via the spectrophotometric analysis of indophenol blue, following the method of Solórzano [27,28] (see Supplementary Materials). Absorbance measurements were made at 660 nm using the Biotek Cytation 5 plate reader.

Potassium, iron, and copper concentrations in the aqueous phase were measured using inductively coupled plasma-optical emission spectrometry (ICP-OES; Varia/Agilent 725 ES; Mulgrave, Victoria, Australia) following dilution in 5% HNO₃(aq) and four-level calibration using certified standard solutions purchased from Inorganic Ventures (Christiansburg, VA, USA).

A Fisherbrand Acument AB15 benchtop pH meter (Fisher Scientific, Pittsburgh, PA, USA) was calibrated with standard solutions and used for all pH measurements. Elemental compositions of metal-loaded materials were characterized using X-ray fluorescence (XRF; PANalytic Zetium).

3.3. Polymer Synthesis

For the synthesis of poly(acrylic acid), a 30 wt% acrylic acid aqueous solution was prepared, and the corresponding molar ratio (1%, 2%, 5%, and 8%, relative to acrylic acid) of crosslinker N-N'-methylbisacrylamide was added to the solution. Initiator 2,2'-azobis(2-methylpropionamidine) dihydrochloride was added to the solution at a concentration of 0.1 wt% relative to acrylic acid. The solution was purged with nitrogen for 5 min, then sealed and incubated at 70 °C for 8 h. The resulting cross-linked hydrogel was ground into small particles and washed with 0.1 M HCl three times (incubating for 4 h, then filtered each time). The washed material was then lyophilized and further ground after lyophilization.

This procedure was also followed for the synthesis of poly(vinylsulfonic acid) with the following exceptions: the monomer utilized was sodium vinyl sulfonate, the cross-linker was dissolved in DMF/H₂O solution prior to addition, and 1 M HCl was used to wash the material five times to provide the acid form of the resin.

3.4. Metal Loading

Moreover, 1.1 M Fe(SO₄) and Cu(SO₄) aqueous solutions were prepared and approximately 2 g of acidic adsorbent was added into 20 mL of solution and stirred for 3 h before replacing the solution. This was repeated at least three times and then washed thoroughly in cycles of 15–20 mL of water followed by filtration until no color could be found on the filter paper. The material was then dried under vacuum at 50 °C overnight. (See Supplementary Materials for XRF data). Zeolite 4A was exchanged with a 10 wt% copper nitrate solution, using 10 cm³/g of zeolite. Exchange was carried out at 90 °C with stirring for 1 h for three cycles, with filtration between each.

3.5. Ammonia and Potassium Capacity Experiment

A 0.05 g sample was placed in 5 mL of 50 mM solution of the relevant ion and placed on a Scilogex SCI-T6-S roller at 70 rpm for 48 h. Samples were then centrifuged, and the supernatant was analyzed, with the exception of poly(acrylic acid-co-maleic acid), where dialysis tubes were used. The starting ammonia concentration was chosen as a 1000-fold excess over the maximum healthy concentration of ammonia in the blood (50 μM), acknowledging a concentration gradient for colon absorption [2] and the threshold concentration for clinical diagnosis (300 μM) [29]. Potassium capacity experiments were conducted in a 50 mM equimolar NH_4Cl and KCl solution.

3.6. Uncertainty Assessment/Statistical Methods

Uncertainty for discreet measurements is estimated as $U_A = k_c \times \frac{SSD}{\sqrt{n}}$, where k_c is the coverage factor determined from the two-tailed inverse of the Student's t -distribution at the 95% confidence interval, SSD is the sample standard deviation and \sqrt{n} is the square root of the number of samples. For most of the data reported, $n = 3$, leading to a rather large coverage factor. Accordingly, the uncertainties are reported at a higher level than would be expected with larger sampling. Further, comparison of control and experimental data sets was conducted using the two-tailed, paired Student's t -test as a default, but in cases where unequal sample sizes were present, homoscedastic distributions were assumed. The p -values generated in these tests were deemed to indicate significant distributions for $p < 0.05$. In charts with more than two sets of data in a given solution, each modified value was compared to the unmodified (control) value. In charts without an indication of p -value, the sample size was too small, and the tests were deemed screening data sets. Student's t -tests and regression analyses to generate p -values were all conducted in Excel[®] 365 version 2308.

4. Conclusions

Many acidic adsorbent materials evaluated as potential hyperammonemia treatments are effective for the adsorption of ammonia, but most are insufficiently selective for adsorption of ammonia over potassium to have therapeutic potential.

Aside from selective adsorption, acidification via non-adsorbable polymeric acids was evaluated as a mode of action and an alternative to lactulose digestion for treating hyperammonemia. By testing various acids in buffered simulated intestinal fluid, it was shown that poly(maleic acid), with its high acid-site density, reduced pH more effectively than simulated lactulose digestion products and with a lower predicted dose. While in vitro studies have yet to be conducted, PMA does have the potential for reduced gastrointestinal side effects, since it is not a sugar and may increase the addressable patient population, including those affected by galactosemia and diabetes. Future research will characterize PAACMA's and PMA's effective doses and side effects.

Supplementary Materials: The following supplementary material can be downloaded at: <https://www.mdpi.com/article/10.3390/ddc2040040/s1>, Equation (S1): Approximate dosage calculation; Table S1: Elemental Composition of Cu-PAA; Table S2: Elemental Composition of Cu-C100EH; Table S3: Elemental Composition of Fe-PAA; Table S4: Elemental Composition of Fe-C100EH; Figure S1: Ammonia equilibrium capacity as a function of cross-linking of PAA; Figure S2: Berthelot reaction; Figure S3: Standard curve for ammonia concentration using Berthelot's reaction; Figure S4: Ammonia equilibrium capacities of PVSA and PAA; Figure S5: Changes in pH caused by PVSA and PAA in aqueous ammonia solutions; Figure S6: Potassium equilibrium capacities of PVSA and PAA in 50 mM NH_4Cl , 50 mM KCl solution. Refs. [2,27,29] are cited in the Supplementary Materials. Notably the threshold concentration for acute hyperammonemia is described as 300 μM based on clinical data [29].

Author Contributions: B.N.: methodology, validation, formal analysis, investigation, resources, data curation, writing—original draft, visualization. C.J.B.: conceptualization, writing—review and editing, supervision, project administration, funding acquisition. M.B.S.: resources, supervision. D.R.C.: resources, supervision. S.V.M.: methodology, resources, writing—review and editing. J.Q.: conceptualization, resources. K.J.S.: investigation, resources. A.M.A.: conceptualization, methodology, writing—review and editing, supervision, project administration, funding acquisition. All authors have read and agreed to the published version of the manuscript.

Funding: This work was funded under a sponsored-research agreement by Bond Biosciences, Inc.

Institutional Review Board Statement: Not applicable.

Informed Consent Statement: Not applicable.

Data Availability Statement: Data are contained within the article.

Conflicts of Interest: The authors declare that C.J.B. is an owner and chief executive officer of Bond Biosciences.

References

1. Ali, R.; Nagalli, S. *Hyperammonemia*; StatPearls Publishing: Treasure Island, FL, USA, 2022.
2. Liu, J.; Lkhagva, E.; Chung, H.-J.; Kim, H.-J.; Hong, S.-T. The Pharmabiotic Approach to Treat Hyperammonemia. *Nutrients* **2018**, *10*, 140. [CrossRef] [PubMed]
3. Weiner, I.D.; Verlander, J.W. Role of NH₃ and NH₄⁺ Transporters in Renal Acid-Base Transport. *Am. J. Physiol. Ren. Physiol.* **2011**, *300*, F11–F23. [CrossRef] [PubMed]
4. Charmot, D. Non-Systemic Drugs: A Critical Review. *Curr. Pharm. Des.* **2012**, *18*, 1434–1445. [CrossRef] [PubMed]
5. Yin Win, K.; Feng, S.-S. Effects of Particle Size and Surface Coating on Cellular Uptake of Polymeric Nanoparticles for Oral Delivery of Anticancer Drugs. *Biomaterials* **2005**, *26*, 2713–2722. [CrossRef] [PubMed]
6. Chaitman, M.; Dixit, D.; Bridgeman, M.B. Potassium-Binding Agents for the Clinical Management of Hyperkalemia. *Pharm. Ther.* **2016**, *41*, 43–50.
7. Center for Drug Evaluation and Research. Drug Trials Snapshots: LOKELMA. FDA 2020. Available online: <https://www.fda.gov/drugs/drug-approvals-and-databases/drug-trials-snapshots-lokelma> (accessed on 9 May 2022).
8. Bond Biosciences. A Phase Ia/Ib Randomized, Double-Blind, Placebo-Controlled, Single and Multiple Ascending Dose Study to Evaluate the Safety, Tolerability and Pharmacodynamics of BBI-001 in Iron Deficient Volunteers and HH Patients; Clinical trial registration NCT05238207. 2022. Available online: <https://clinicaltrials.gov> (accessed on 8 May 2022).
9. Science & Pipeline. Ardelyx. Available online: <https://ardelyx.com/science-pipeline/> (accessed on 9 May 2022).
10. Ardelyx, Inc. Ardelyx Receives FDA Approval for IBSRELA®(Tenapanor), an NHE3 Sodium Transport Inhibitor, for the Treatment of Irritable Bowel Syndrome with Constipation. Available online: <https://ir.ardelyx.com/news-releases/news-release-details/ardelyx-receives-fda-approval-ibsrelar-tenapanor-nhe3-sodium> (accessed on 13 May 2022).
11. Cuartero, M.; Colozza, N.; Fernández-Pérez, B.M.; Crespo, G.A. Why Ammonium Detection Is Particularly Challenging but Insightful with Ionophore-Based Potentiometric Sensors—An Overview of the Progress in the Last 20 Years. *Analyst* **2020**, *145*, 3188–3210. [CrossRef] [PubMed]
12. Clark, B.; Tarpeh, W.A. Selective Recovery of Ammonia Nitrogen from Wastewaters with Transition Metal-Loaded Polymeric Cation Exchange Adsorbents. *Chem. A Eur. J.* **2020**, *26*, 10099–10112. [CrossRef] [PubMed]
13. Patil, D.H.; Westaby, D.; Mahida, Y.R.; Palmer, K.R.; Rees, R.; Clark, M.L.; Dawson, A.M.; Silk, D.B. Comparative Modes of Action of Lactitol and Lactulose in the Treatment of Hepatic Encephalopathy. *Gut* **1987**, *28*, 255–259. [CrossRef] [PubMed]
14. Mukherjee, S.; John, S. *Lactulose*; StatPearls Publishing: Treasure Island, FL, USA, 2021.
15. Budavari, S. *The Merck Index: An Encyclopedia of Chemicals, Drugs, and Biologicals*, 11th ed.; Merck: Rahway, NJ, USA, 1989.
16. Tasić, Ž.; Bogdanović, G.; Antonijević, M. Application of Natural Zeolite in Wastewater Treatment: A Review. *J. Min. Metall. A Min.* **2019**, *55*, 67–79. [CrossRef]
17. Weatherley, L.R.; Miladinovic, N.D. Comparison of the Ion Exchange Uptake of Ammonium Ion onto New Zealand Clinoptilolite and Mordenite. *Water Res.* **2004**, *38*, 4305–4312. [CrossRef] [PubMed]
18. Han, B.; Butterly, C.; Zhang, W.; He, J.; Chen, D. Adsorbent Materials for Ammonium and Ammonia Removal: A Review. *J. Clean. Prod.* **2021**, *283*, 124611. [CrossRef]
19. Adam, M.R.; Othman, M.H.D.; Abu Samah, R.; Puteh, M.H.; Ismail, A.F.; Mustafa, A.; Rahman, M.A.; Jaafar, J. Current Trends and Future Prospects of Ammonia Removal in Wastewater: A Comprehensive Review on Adsorptive Membrane Development. *Sep. Purif. Technol.* **2019**, *213*, 114–132. [CrossRef]
20. Hoffman, M. The Intestines (Human Anatomy): Picture, Function, Location, Parts, Definition, and Conditions. Available online: <https://www.webmd.com/digestive-disorders/picture-of-the-intestines> (accessed on 27 April 2022).
21. Booker, N.A.; Cooney, E.L.; Priestley, A.J. Ammonia Removal from Sewage Using Natural Australian Zeolite. *Water Sci. Technol.* **1996**, *34*, 17–24. [CrossRef]

22. Aydin, F.; Zhan, C.; Ritt, C.; Epsztein, R.; Elimelech, M.; Schwegler, E.; Pham, T.A. Similarities and Differences between Potassium and Ammonium Ions in Liquid Water: A First-Principles Study. *Phys. Chem. Chem. Phys.* **2020**, *22*, 2540–2548. [[CrossRef](#)] [[PubMed](#)]
23. Marques, M.R.C.; Loebenberg, R.; Almukainzi, M. Simulated Biological Fluids with Possible Application. *Dissolut. Technol.* **2011**, *18*, 15–28. [[CrossRef](#)]
24. Chitanu, G.C.; Rinaudo, M.; Desbrières, J.; Milas, M.; Carpov, A. Behavior of Nonalternating Maleic Acid Copolymers in Aqueous Solution. *Langmuir* **1999**, *15*, 4150–4156. [[CrossRef](#)]
25. Robson, H. Method for Preparing a Small Pore Synthetic Zeolite. U.S. Patent 3,720,753A, 13 March 1973.
26. Robson, H.E. Zeolite RHO. U.S. Patent 3,904,738A, 9 September 1975.
27. Zhu, Y.; Chen, J.; Yuan, D.; Yang, Z.; Shi, X.; Li, H.; Jin, H.; Ran, L. Development of Analytical Methods for Ammonium Determination in Seawater over the Last Two Decades. *TrAC Trends Anal. Chem.* **2019**, *119*, 115627. [[CrossRef](#)]
28. Solórzano, L. Determination of Ammonia in Natural Waters by the Phenolhypochlorite Method. *Limnol. Oceanogr.* **1969**, *14*, 799–801. [[CrossRef](#)]
29. Savy, N.; Brossier, D.; Brunel-Guitton, C.; Ducharme-Crevier, L.; Du Pont-Thibodeau, G.; Jovet, P. Acute pediatric hyperammonemia: Current diagnosis and management strategies. *Hepatic Med.* **2018**, *10*, 105. [[CrossRef](#)] [[PubMed](#)]

Disclaimer/Publisher's Note: The statements, opinions and data contained in all publications are solely those of the individual author(s) and contributor(s) and not of MDPI and/or the editor(s). MDPI and/or the editor(s) disclaim responsibility for any injury to people or property resulting from any ideas, methods, instructions or products referred to in the content.